Collection of Carbon Particles in Diesel Exhaust Gas Using Intermittent Dielectric Barrier Discharge

Keiichiro YOSHIDA

Osaka Institute of Technology, Osaka, Japan
keiichiro.yoshida@oit.ac.jp

Abstract. This study investigated the performance of a novel electrostatic precipitator. This system consists of a charging section and collection section with glass plates that have discharge electrodes on them. Biased alternating current (AC) with high voltage was intermittently applied to the discharge electrodes to build up charges with polarity similar to the bias on the dielectric surface to create a strong electric field between the electrodes and the surface. This electric field attracts the soot charged in the charging section to the glass surface, where plasma can cause the oxidative decomposition of the collected soot. In this system, the intermittent mode of voltage application plays a key role in the collection of particulates. The collection efficiency of the reactor was estimated with an OFF duration in the range of 0–1990 ms and an ON duration of 10 ms. The surface potential distributions of the dielectric substrates used in the reactor were measured with respect to the time duration after the voltage application had been completed. Thus, it was found that the collection efficiency was influenced by the OFF duration, because the surface charges on the glass plates had a certain lifetime.

Keywords: Soot, Carbon particle, $PM_{2.5}$, Surface potential, Diesel engine, Exhaust gas, Dielectric barrier discharge

1 INTRODUCTION

In many regions worldwide, the concentration of $PM_{2.5}$, whose particulate matter (PM) aerodynamic diameter does not exceed 2.5 μm, largely surpasses the value of 25 $\mu g/m^3$ recommended by the World Health Organization [1, 2]. These particles

often originate from human activity. Carbon particulates from combustion processes are a potential risk to human health because they generally consist of many primary particles with a diameter of approximately 0.1 μm and harmful hydrocarbons that are adsorbed between the primary particles. Therefore, carbon particulates must be removed from the exhaust gases of combustion devices and from the atmosphere. Diesel particulate filters (DPFs) have been used as a technique for the aftertreatment of gas exhausted by diesel engines. However, the pressure loss and additional energy consumption of DPFs must still be mitigated. Electrostatic precipitation is a promising technology for reducing the carbon particulates produced by engines and those in the atmosphere, because it consumes less energy and provides small pressure drop. Therefore, several aftertreatment techniques have been intensively developed [3-18]. The authors previously investigated a novel type of electrostatic precipitator, by which particulates are first adhered to a dielectric surface that is regularly decomposed by a dielectric barrier discharge (DBD) plasma [19, 20]. This technique consumes a small amount of energy because the regeneration process using the DBD plasma is only conducted occasionally. Fig.1 shows the collection mechanism assumed by previous studies [19, 20]. The high-voltage that is intermittently applied to the discharge electrodes on the dielectric surface results in a high surface potential after the voltage application has been completed. The electric field created between the surface and the discharge electrode guides the particles that are charged in advance with opposite polarity at the charging section. This study investigated the relationships among the time interval between voltage applications, the particulate collection efficiency, and the surface potential.

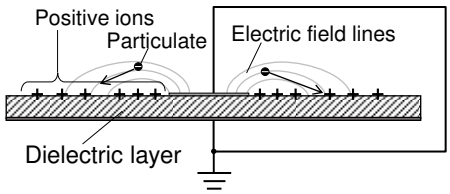

Fig. 1. Particle collection mechanism.

2 EXPERIMENTAL SETUP AND METHOD

Fig. 2 shows the internal structure of the aftertreatment device that removes the PM from the exhaust gas. A 25-mm long charging section and a 125-mm long collection section were placed in series in an acrylic chamber. In the charging section, three needles (diameter of 0.5 mm) made of stainless steel were used as the corona discharge electrodes. Negative direct current (DC) with high voltage was applied to provide passing particles with negative charges.

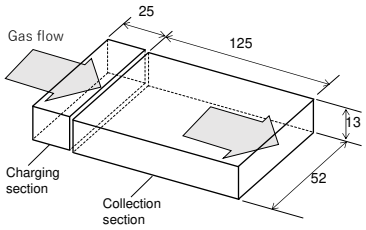

Fig. 2. Internal structure of PM reactor.

Fig. 3 shows the electrode plates comprising the collection section. As shown in Fig. 3(a), one of the electrode plates consisted of a borosilicate glass plate with a thickness of 1.3 mm, a discharge electrode pattern made of copper film, and a ground electrode attached behind the glass plate. The discharge electrode consisted of four strips with a width of 2.5 mm placed at an interval of 8 mm. Fig. 3(b) shows the four electrode plates stacked in the collection section. The gas stream was divided into two channels with a height of 3.6 mm, which were formed by surfaces with discharge electrodes.

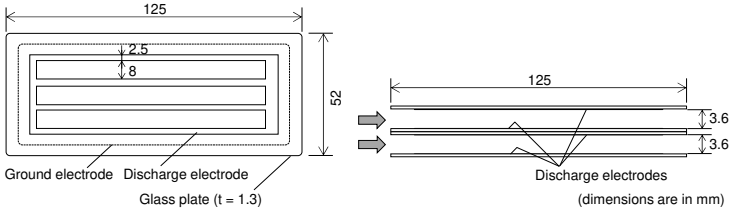

(a) Top view of electrode plate (b) Side view of stacked electrode plates.

Fig. 3. Electrode plates for particle collection.

Fig. 4 shows the experimental setup used to test the performance of the PM reactor. A stationary diesel engine generator (YDG200VS, Yanmar Diesel Co. Ltd.; displacement=200 mL, rotation rate=3600 rpm, load rating=2 kW) was used as the particulate source, and a 1-kW electric heater was connected to it as the load. The exhaust gas contained O_2, CO, NO, and NO_2 gas components at the volume concentrations of 12.6–12.7%, 360–430 ppm, 230–260 ppm, and 20–30 ppm, respectively, and PM of 20–25 mg/m^3. Part of the exhaust gas was introduced into the PM reactor, which was placed in a thermostatic chamber maintained at 70 °C. The gas immediately downstream of the reactor was branched into a glass fiber filter (Advantec Co., Ltd., GF-75; filtration efficiency of 0.3 μm, particle diameter>99.999%) to quantify the PM concentration. The branching flow rate was precisely controlled at 7 L/min using a mass-flow controller. After the PM sampling port, the gas flow rate was measured using the difference between the static and dynamic flow pressures at a flow bench. A single performance test consisting of five 20-minute PM samplings was conducted in series at one-minute intervals. The PM reactor was operated during the third and fourth turns of the sampling (operated for 41 min). The PM removal performance of the reactor was determined by comparing the PM

concentrations downstream of the reactor measured at the time when the reactor was operated and the time when the reactor was not operated.

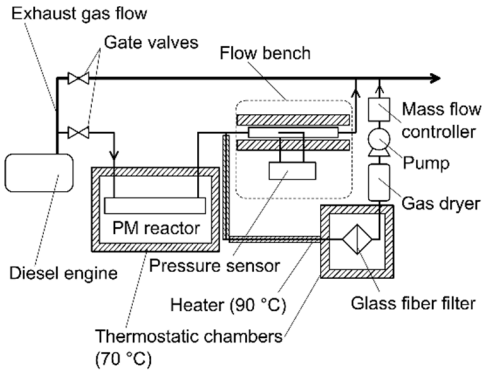

Fig. 4. Setup for testing performance of PM reactor.

Two types of PM removal efficiencies, namely, η_t and η_{ch}, are defined in Equations (1) and (2).

$$\eta_{\mathrm{t}} = 1 - \frac{C_1}{C_0} \tag{1}$$

$$\eta_{\mathrm{ch}} = 1 - \frac{C_{\mathrm{m}}}{C_0} \tag{2}$$

where η_t is the efficiency of the entire reactor and η_{ch} is the efficiency of only the charging section; C_0 is the PM concentration when the reactor was not operated and C_1 is the PM concentration when the reactor was operated; C_m is the PM concentration immediately after the charging section, and is not a measured value but rather a value deduced from the weight change of the charging and collection section.

Fig. 5 shows the electric circuit used to apply high voltage to the discharge electrodes of the collection section. A voltage that oscillated from 0 to the positive maximum was generated by shifting a 10-kHz AC voltage from a power source (Masuda Research Inc., LC-SDBD-100; controllable with external on/off signals) by its amplitude using a circuit comprising a capacitor and a diode. The 50-MΩ resistor connected in parallel to the diode quickly returned the voltage to 0 V when the AC high voltage was turned off. The current flowing through the collection section was detected as the voltage at the 100-Ω resistor inserted between the AC power source and the ground.

Fig. 6(a) shows the typical waveforms of the voltage applied to the discharge electrodes at the collection section. The voltage was alternately ON and OFF for a regular period. The ON and OFF durations are indicated as t_{on} and t_{off}, respectively.

When the AC voltage was turned off, it took approximately 100 ms for the voltage to return to 0 V.

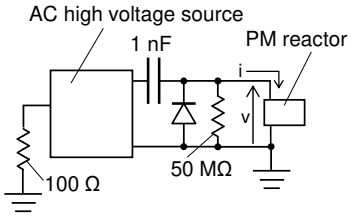

Fig. 5. Electric circuit used to apply high voltage to collection section.

Fig. 6(b) shows the applied voltage and current i that flowed through the collection section during the ON period. As can be seen, the voltage varied from 0 to the positive maximum. The power consumed in the collection section can be calculated as follows:

$$P_{\mathrm{on}} = \frac{1}{nT}\int_{t_0}^{t_0+nT} ivdt \tag{3}$$

$$P = P_{\mathrm{on}} \times \frac{t_{\mathrm{on}}}{t_{\mathrm{on}} + t_{\mathrm{off}}} \tag{4}$$

where P_{on}, i, v, and T represent the instant power, current, voltage, and AC voltage period during the ON period; n is the number of periods in the obtained data; t_0 simply indicates the beginning of integration. The average value of P_{on} was approximately 16 W. The power consumed at the collection section P was determined using Equation (4) and P_{on}. The power dissipation at the bias circuit is not included in P.

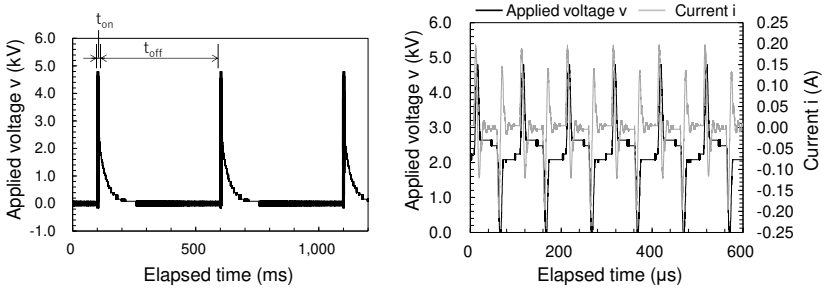

(a) ON-OFF pattern (b) Waveform of ON duration.

Fig. 6. Typical waveforms of voltage applied to collection section.

Fig. 7 describes the method for measuring the surface potential on the electrode plate. Because the potential difference between the dielectric surface and the discharge electrodes during the OFF period is a key consideration in this technique, the change in the surface potential was measured after the voltage application had been completed. To investigate the potential decay under a realistic condition, the electrode plates that had been used in the PM reactor for 20 minutes (half the operating duration of a typical PM treatment test) were used in the measurement. A noncontact voltmeter (Trek Inc., model 347; measurement range: 0 – ±3 kV, response time (10%–90%) < 3 ms for a step change of 1 kV) was used to measure the surface potential. The tip of the potential probe was kept at a distance of 8 mm from the surface to avoid interference with the discharge during the ON periods. Immediately after the ON and OFF periods had been repeated 10 times, the tip of the probe was quickly moved to a distance of 1 mm from the surface using a servo motor controlled by a microcomputer. The changes in the potential after 200 ms from the start of the OFF period were observed.

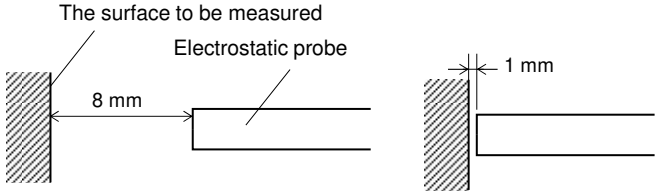

(a) While voltage was applied (b) While the surface potential was measured.

Fig. 7. Method for measuring surface potential.

3 RESULTS AND DISCUSSION

Fig. 8 shows the PM removal efficiencies η_t and η_{ch} as functions of the OFF duration t_{off}, which was changed from 0–1990 ms with t_{on} fixed at 10 ms. The flow rate of the exhaust gas was 35 NL/min. A DC voltage of −4.2 kV was applied to the corona needles of the charging section, and as a result, a current of 160 μA flowed to charge the particles. The value of η_{ch} was approximately 0.28, regardless of t_{off}, owing to the constant condition in the charging section. Moreover, η_t exhibited an approximate peak value of 0.78 when t_{off} was approximately 490 ms. This result can be explained by the potential difference between the discharge electrodes and the glass surface. The surface potential of the dielectric plate decreased as t_{off} increased. However, with an extremely small t_{off}, the period wherein the discharge electrodes were at high potential occupied a larger part of the repetition period (t_{on}+t_{off}). Therefore, the time average of the potential difference likely reached the maximum with t_{off}≈500 ms, yielding the highest η_t. Additionally, when t_{off} was 0 ms (voltage was continuously applied), the particulates were guided directly onto the discharge elec-

trodes owing to the electric field formed between the charging section and the discharge electrodes [20]. The above results suggest that the surface potential decayed with a time constant in the order of 0.5 s.

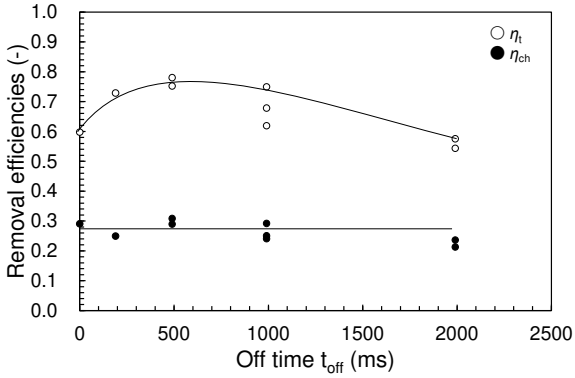

Fig. 8. Particulate removal efficiencies as functions of t_{off}.

Fig. 9 shows the area wherein the surface potentials were measured. Specifically, the figure shows the electrode plate that was used in the PM reactor under the same conditions as those of the reactor performance test for 20 minutes, and indicates that the particulates adhered intensively to the area surrounding the discharge electrodes, which suggests that the negatively charged particles were guided by the positive charges on the glass substrate. As can be seen, the particulate adhesion is denser at the upper stream part. The x-axis and y-axis are defined to indicate the locations on the substrate; the x-axis is defined along the direction of the gas stream with x=0 at the upstream end; Δy measures the distance from the edge of one of the electrode strips toward the middle of the interval between the electrode strips. The surface potentials were measured at locations in the range of 5 mm ≤ x ≤ 50 mm and −0.5 mm ≤ y ≤ 4.0 mm at increments of 0.5 mm.

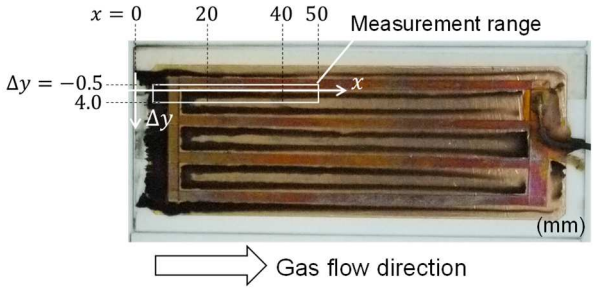

Fig. 9. Electrode plate used in PM reactor and area wherein the surface potential was measured.

The time series data for the surface potential V_s were reordered into space distributions. Figs. 10(a) and (b) show the distributions of V_s at x=40 mm and 20 mm, respectively, for the time range from the start of the OFF duration, that is, 200–4000

ms. The surface potentials decayed with time for all locations. Notably, V_s was assumed to be 0 V at Δy=0 mm, but the probe obtained information within an area with a width of approximately 1 mm, which resulted in non-zero potentials.

For the distributions at x=40 mm at 200 ms, V_s was approximately 1700 V and 2100 V at Δy=0.5 mm and 1.0 mm, respectively, and reached the maximum of 2150 V at Δy=1.5 mm. The maximum potential gradient along the surface was 3.4 MV/m, which exceeds the dielectric strength of air. Considering the low spatial resolution of the probe, it was assumed that the potential gradient reached the limitation of 3 MV/m. For the distributions at x=20 mm at 200 ms, V_s was 1200 V and 1850 V at Δy=0.5 mm and 1.0 mm, respectively, and reached the maximum of 2100 V at Δy=2.0 mm. The maximum potential gradient was 2.4 MV/m, which is lower than that for x=40 mm. The lower gradient is attributed to the denser deposition of particulates at x=20 mm compared with x=40 mm. However, the maximum potentials were the same when Δy was sufficiently large.

For Δy=1.0 mm at 4000 ms, V_s was 1500 V and 1200 V at x=40 mm and 20 mm, respectively. These values are 71% and 65% of those at 200 ms at each x location, which indicates that the more densely deposited particulates accelerated the potential decay.

With a clean surface, the surface potential increased up to the time-average of the applied voltage of 2500 V [20] and maintained its value for more than several minutes [21]. Hence, the above results suggest that the conductivity of the deposited particulates allows the absorption of surface charges by the discharge electrodes.

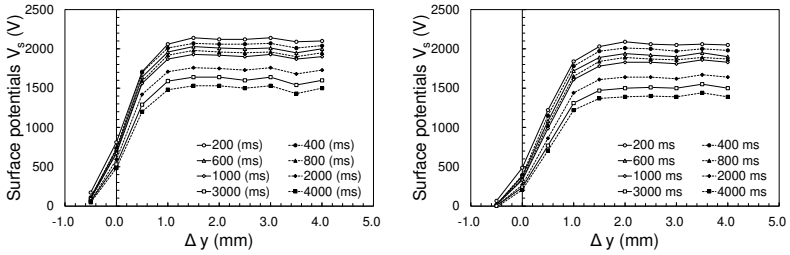

(a) At x=40 mm (b) At x=20 mm

Fig. 10. Change in surface potential distributions.

Based on the mechanism described in Fig. 1, the time-average of the difference between the surface potential and that of the discharge electrode $\overline{V_s - v}$ expressed by Equation (5) determines the PM removal efficiency at the collection section.

$$\overline{V_s - v} = \frac{1}{t_{on} + t_{off}} \int_0^{t_{on}+t_{off}} (V_s - v) dt \tag{5}$$

Fig. 11 shows $\overline{V_s - v}$ as a function of t_{off}. The calculations were carried out with a potential difference of 0 V during the ON period, and V_s at $t=t_{on}$ + 200 ms was used

for t from t_{on} to t_{on} + 200 ms. Therefore, $\overline{V_s - v}$ was 0 V at t_{off}=0, rapidly increased up to its maximum at t_{off}≈600 ms, and subsequently decreased slowly for a larger t_{off} at either x=20 mm or 40 mm. These results are almost consistent with the fact that η_t peaked at t_{off}=490 ms. However, η_t appears to have decreased more rapidly than $\overline{V_s - v}$ after they reach the respective peaks. This discrepancy is attributed to the higher relative humidity and temperature of the exhaust gas, whereby the surface charges would have dissipated more rapidly.

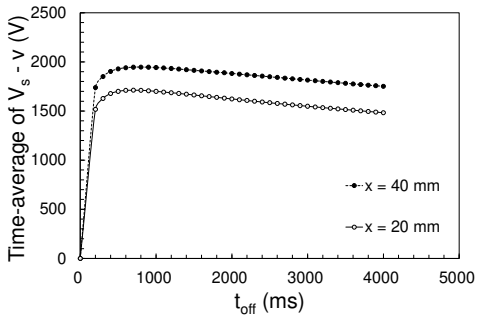

Fig. 11. Time-average of potential differences between dielectric substrate and electrode, $\overline{V_s - v}$.

4 CONCLUSIONS

Applying intermittent unipolar high voltage to discharge electrodes on dielectric substrates creates a potential distribution whereby the dielectric surface has high voltages and the discharge electrodes are at 0 V. To elucidate the particle collection mechanism in this technique using the uneven potential distribution, the relationship between the potential variation on the surface of the dielectric substrate and the particle removal efficiency of the reactor was investigated. The gas exhausted by a diesel engine was used as the particulate source. The voltage applied to the discharge electrodes in the collection section was generated by shifting a 10-kHz AC high voltage such that it oscillated between 0 and +5 kV. The OFF duration t_{off} was varied from 0 to 1990 ms with the ON duration fixed at 10 ms. The surface potentials were measured for the substrate with particulate deposition. The following conclusions were drawn from the experimental results:

(a) The maximum particulate removal efficiency of 0.78 was achieved when t_{off} was 490 ms.

(b) The surface potential gradient along the surface decreased as the density of the deposited particulates increased, but exceeded 3 MV/m at a part with relatively less dense particulates. For locations at a sufficient distance from the electrode edge, the potential values were slightly lower than the time-average of the voltage applied to the electrode, regardless of the particulate deposition density. The

decay of the potential was accelerated by the particulate. By comparing the values at the distance of 1 mm from the electrode edge, it was found that the decay was 71% and 65% of the initial values in 4 s at locations with relatively less and more particulate deposition, respectively. These results suggest that the surface charges were absorbed by the electrodes owing to the conductivity of the deposited particulates.

(d) The potential difference between the dielectric substrate and the electrode time-averaged over the ON and OFF periods reached its maximum at t_{off}=600 ms. This result indicates that the potential difference determines the reactor performance.

Acknowledgements

This study was supported by the Steel Foundation for Environmental Protection Technology, and a JSPS KAKEN Grant-in-Aid for Scientific Research (C) (Grant No. JP18K11702). The author is grateful to undergraduate students Sayato KUZE and Tetsu MISHIMA for their assistance in the experiments.

REFERENCES

1. van Donkelaar, A.*, et al.* (2010) Global estimates of ambient fine particulate matter concentrations from satellite-based aerosol optical depth: development and application. Environmental Health Perspectives 118: 847-55. doi:10.1289/ehp.0901623
2. Warneck, P. and Williams, J. in *The atmospheric chemist's companion: numerical data for use in the atmospheric sciences* Ch. 5 The Atmospheric Aerosol, pp 127-187 (2012).
3. Yamamoto, T.*, et al.* (2010) Diesel PM Collection for Marine and Automobile Emissions Using EHD Electrostatic Precipitators. IEEE Transacntions on Industry Applications 46: 1606-1612.
4. Yamamoto, T.*, et al.* (2009) Electrohydrodynamically Assisted Electrostatic Precipitator for the Collection of Low-Resistivity Dust. IEEE Transacntions on Industry Applications 45: 2178-2184.
5. Takasaki, M.*, et al.* (2015) Electrostatic Precipitation of Diesel PM at Reduced Gas Temperature. In: 2015 IEEE Industry Applications Society Annual Meetig. Dallas, Texas, U.S., pp 2015-EPC-0498.
6. Yamamoto, T., Maeda, W., Ehara, Y. and Kawakami, H. (2011) Development of EHD-Enhanced Plasma Electrostatic Precipitator. In: IEEE-IAS Annual Meeting. Orlando, Florida, U. S., pp Total 7 pages.
7. Gouri, R., Zouzou, N., Tilmatine, A., Moreau, E. and Dascalescu, L. (2011) Collection of submicron particles using DBD electrostatic precipitator in wire-to-square tube configuration. In: 13th International Conference on Electrostatics. Bangor which is located in North West Wales, pp 012012.

8. Dramane, B., Zouzou, N., Moreau, E. and Touchard, G. (2009) Electrostatic Precipitation of Submicron Particles using a DBD in Axisymmetric and Plannar Configurations. IEEE Transactions on Dielectrics and Electrical Insulation 16: 343-351.
9. Byeon, J. H.*, et al.* (2006) Collection of submicron particles by an electrostatic precipitator using a dielectric barrier discharge. Journal of Aerosol Science 37: 1618-1628.
10. Kawada, Y.*, et al.* (1999) Development of High Collection Efficiency ESP by Barrier Discharge System. In: IEEE 34th Annual Meeting of the IEEE Industry Applications. Phoenix, AZ, USA, pp 1130-1135.
11. Kawai, Y.*, et al.*, *Industrial Plasma Technology -Applications from Environmental to Energy Technologies-*. Wiley-VCH: 2010; Vol. Weinheim, Germany, p 434.
12. Yamasaki, H.*, et al.* (2020) In-flight diesel particulate matter removal using nonthermal plasma filtering. International Jounal of Plasma Environmental Science and Technology 14: e03007. doi:10.34343/ijpest.2020.14.e03007
13. Yamamoto, S.*, et al.* (2009) Pulsed plasma PM removal from diesel exhaust emissions. Influences of reaction conditions. Electrochemistry 77: 1013-1017.
14. Zouzou, N., Ndong, A. C. A. a. and Moreau, E. (2017) Regeneration of Sooty Surace Using Nanosecond Pulsed Dielectric Barrier Discharge. IEEE Transacntions on Industry Applications 53: 3982-3988.
15. Yao, S., Madokoro, K., Fushimi, C. and Fujioka, Y. (2007) Experimental Investigation on Diesel PM Removal Using Uneven DBD Reactors. Environmental and Energy Engineering 53: 1891-1897.
16. Fushimi, C., Madokoro, K., Yao, S., Fujioka, Y. and Yamada, K. (2008) Influence of Polarity and Rise Time of Pulse Voltage Waveforms on Diesel Particulate Matter Removal Using an Uneven Dielectric Barrier Discharge Reactor. Plasma Chem Plasma Process 28: 511-522.
17. Ehara, Y.*, et al.* (2013) Diesel PM incineration for marine emissions using dielectric barrier discharge type electrostatic precipitator. In: ESA Annual Meeting on Electrostatics 2013. Cocoa Beach, Florida, U. S., pp 8 pages.
18. Adachi, M.*, et al.* (2001) Characteristics of Electrode Length and Mean Gas Velocity with Barrier Discharge Type ESP. In: The European Aerosol Conference. pp s944-s943.
19. YOSHIDA, K. (2021) Collection of Particulate Matters in Diesel Exhaust Gas by Uneven Potential Distribution Created along a Dielectric Surface. In: IEEE-IAS Annual Meeting 2021. Virtual (Initial location: Vancouver, BC, Canada), pp 1-6.
20. YOSHIDA, K. (2022) Collection of Particulate Matters in Exhaust Gas Using the Attractive Force Induced by Surface Charging. IEEE Transacntions on Industry Applications 58: 2462-2470. doi:10.1109/TIA.2022.3141042
21. Ricchiuto, R. C., Borghi, C. A., Cristofolini, A. and Neretti, G. (2020) Measurement of the charge distribution deposited on a target surface by an annular plasma synthetic jet actuator: Influence of humidity and electric field. Journal of Electrostatics 107: 103501.